Complex Low Energy Tetrahedral Polymorphs of Group IV Elements from First Principles

Chaoyu He,[1,2,*] Xizhi Shi,[1,2] S. J. Clark,[3] Jin Li,[1,2] Chris J. Pickard,[4,5,†] Tao Ouyang,[1,2] Chunxiao Zhang,[1,2] Chao Tang,[1,2] and Jianxin Zhong[1,2]

[1]*Hunan Key Laboratory for Micro-Nano Energy Materials and Devices, Xiangtan University, Hunan 411105, People's Republic of China*

[2]*School of Physics and Optoelectronics, Xiangtan University, Xiangtan 411105, China*

[3]*Durham University, Centre for Material Physics, Department of Physics, South Road, Durham, DH1 3LE, United Kingdom*

[4]*Department of Materials Science & Metallurgy, University of Cambridge, 27 Charles Babbage Road, Cambridge CB30FS, United Kingdom*

[5]*Advanced Institute for Materials Research, Tohoku University 2-1-1 Katahira, Aoba, Sendai, 980-8577, Japan*

(Received 12 July 2018; published 26 October 2018)

The energy landscape of carbon is exceedingly complex, hosting diverse and important metastable phases, including diamond, fullerenes, nanotubes, and graphene. Searching for structures, especially those with large unit cells, in this landscape is challenging. Here we use a combined stochastic search strategy employing two algorithms (*ab initio* random structure search and random sampling strategy combined with space group and graph theory) to apply connectivity constraints to unit cells containing up to 100 carbon atoms. We uncover three low energy carbon polymorphs ($Pbam$-32, $P6/mmm$, and $I\bar{4}3d$) with new topologies, containing 32, 36, and 94 atoms in their primitive cells, respectively. Their energies relative to diamond are 96, 131, and 112 meV/atom, respectively, which suggests potential metastability. These three carbon allotropes are mechanically and dynamically stable, insulating carbon crystals with superhard mechanical properties. The $I\bar{4}3d$ structure possesses a direct band gap of 7.25 eV, which is the widest gap in the carbon allotrope family. Silicon, germanium, and tin versions of $Pbam$-32, $P6/mmm$, and $I\bar{4}3d$ also show energetic, dynamical, and mechanical stability. The computed electronic properties show that they are potential materials for semiconductor and photovoltaic applications.

DOI: 10.1103/PhysRevLett.121.175701

The group IV elements carbon and silicon are central to life and technology, respectively. Carbon can form many allotropes in addition to graphite and cubic diamond (cd). For example, quasi-zero-dimensional fullerenes, quasi-one-dimensional nanotubes, quasi-two-dimensional graphene, and other three-dimensional crystals such as hexagonal diamond (hd), chaoite [1–3], and amorphous carbon. In the past decades, hypothetical crystalline structures of carbon [4,5] have been predicted. Some of these structures, such as M carbon [6,7], S carbon [8,9], $C_{20\text{-sc}}$, $C_{21\text{-sc}}$, and $C_{22\text{-sc}}$ [10,11] are believed to have been synthesized in previous experiments [12,13]. Others (such as $P6522$ [14], $P42/ncm$ [15], $Pbam$-24 [16], calt34 [17], and calt46 [17]) also possess better energetic stabilities in comparison with cd and are targets for future experimental synthesis. Some have been reported as experimentally realized crystals, e.g., the monoclinic V carbon [18] was obtained by compressing C70 pea pods and the previously predicted T carbon [19] was recently claimed to have been synthesized through pseudotopotactic conversion of a multiwalled carbon nanotube [20].

Silicon, germanium, and tin adopt similar structures to carbon, and have also attracted many theoretical efforts to explore their polymorphs [15,16,21–30]. Advances accessing silicon polymorphs through unconventional pathways, such as ultrafast laser-induced confined microexplosion [31] and high-pressure precursor routes [32], has increased interest in silicon and germanium [33]. Low energy silicon allotropes with direct-band gaps of the appropriate size are anticipated for future applications to solar-energy conversion [28–30,34].

The development of rapid and reliable codes for the computation of material properties, combined with the advent of algorithms for the prediction of crystal structures [35–38], and an increase in the performance and availability of computational resources allows us to discover new materials from first principles. In this Letter, we report three low-energy tetrahedral polymorphs (identified by their space groups, $Pbam$-32, $P6/mmm$, and $I\bar{4}3d$) for carbon, silicon, germanium, and tin, which are obtained using a stochastic search strategy as implemented in the *ab initio* random structure search (AIRSS) [35,36] and the random sampling strategy combined with space group and graph theory (RG^2) [5]. Density functional theory (DFT) based first-principles calculations as implemented in the Vienna *ab initio* simulation package (VASP) [39] and

CASTEP [52] were employed to investigated their structures, energetic, dynamical, and mechanical stabilities, as well as electronic and mechanical properties. Our results show that these three tetrahedral polymorphs possess remarkable energetic stabilities in carbon, silicon, germanium, and tin, in comparison with those metastable phases previously proposed. They are confirmed to be both dynamically and mechanically stable. The carbon *Pbam*-32, *P*6/*mmm*, and $I\bar{4}3d$ structures are superhard insulators with excellent mechanical properties. In silicon, they are potential absorber materials for thin-film solar-cell applications according to their proper band gaps. Notably, the carbon $I\bar{4}3d$ structure is a wide-gap semiconductor with a 7.25 eV gap, which is believed to be the widest gap in the carbon family.

Perspective views of the carbon *Pbam*-32, *P*6/*mmm*, and $I\bar{4}3d$ structures are shown in Fig. 1. The corresponding structural information is provided in Table S3 of the Supplemental Material [39]. The *Pbam*-32 structure is structurally very similar to the previously proposed *Pbam*-24 structure [16] with fivefold, sixfold, and sevenfold topological carbon rings. *Pbam*-32 and *Pbam*-24 are orthorhombic phases belonging to *Pbam* (No.55) symmetry with 8/32 and 6/24 inequivalent/total carbon atoms in their unit cell, respectively. We find that both *Pbam*-24 and *Pbam*-32 have straightforward transformation paths from graphite (see Fig. S1 [39]) and can be considered as good candidates for explaining the diversity of products on the cold compression of graphite [12]. Their simulated x-ray diffraction patterns (XRD) are provided and compared with the experimental results in Fig. S3 [39], which show that both *Pbam*-32 and *Pbam*-24 can partially explain the experimental XRD.

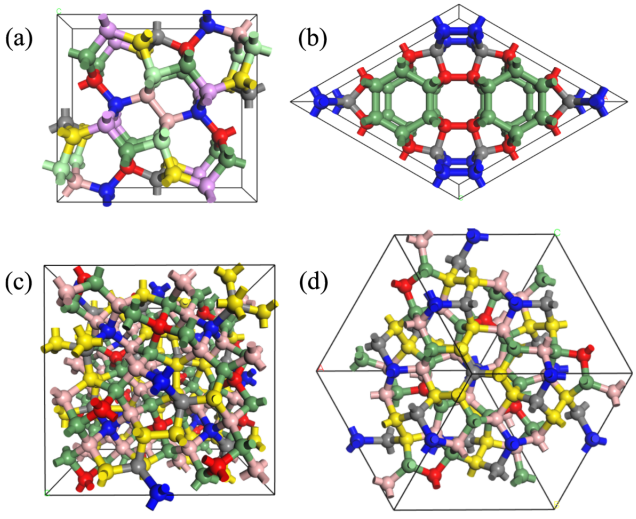

FIG. 1. The perspective crystalline views of the optimized carbon-version *Pbam*-32 (a) and *P*6/*mmm*, (b), as well as those of $I\bar{4}3d$ in both crystalline cell (c) and primitive cell (d). Balls in different colors indicate different inequivalent carbon atoms.

The cold compression of carbon nanotube (CNT) bundles [53] is another route to synthesize novel carbon phases, and is an effective theoretical way to design new carbon crystals [54,55]. The corresponding transition pathways from suitably arranged (4, 0)-CNTs to *Pbam*-32 and *Pbam*-24 are suggested in Fig. S1 [39]. These discoveries indicate that both *Pbam*-24 and *Pbam*-32 may be synthesized by cold compressing graphite [12] and CNTs [53], similar to the *V* carbon (105 meV/atom) recently synthesized by compressing C70 pea pods [18].

The *P*6/*mmm* structure possesses relatively high symmetry (No. 191) in comparison with *Pbam*-32. There are 36 carbon atoms in the crystalline cell of *P*6/*mmm* and only 4 of them are inequivalent. The *P*6/*mmm* structure contains fivefold, sixfold, and eightfold topological carbon rings, which is similar to the previously proposed low-energy M585 phase [56]. A simple pathway for structurally transforming perfect graphite to *P*6/*mmm* is currently unknown. However, it can be structurally transformed from the well-arranged array of (3, 0)-CNTs, (9, 0)-CNTs, and (3, 0)-(9, 0)-CNTs as indicated in Fig. S2 [39]. The *P*6/*mmm* structure, with its relatively low energy as compared to previously proposed post-carbon-nanotube phases [54,55] may be a target for experimental synthesis. As such, we calculate the XRD of *P*6/*mmm* carbon and present it in Fig. S3 of the Supplemental Material [39] for future experimental comparison.

$I\bar{4}3d$ is a topologically interesting cubic carbon phase with very high symmetry (No. 220). It is a complex structure containing 94 carbon atoms in its primitive cell (188 atoms in the conventional cubic cell). Only six of them are inequivalent. Such a large-sized and low-energy carbon structure presents a challenge to crystal structure prediction techniques [35–38]. It was first identified by the RG^2 code [5] and then quickly rediscovered using the newest AIRSS [35,36] code. The carbon rings in $I\bar{4}3d$ are only fivefold, sixfold, and sevenfold, which are different from the previously proposed sp^3 cubic carbons containing threefold, fourfold, sixfold, and eightfold carbon rings. We find no potential pathways for transforming graphite and CNTs to $I\bar{4}3d$ due to its complex network. However, in view of its stability, we might expect it to be discovered in the aerolite [57] or synthesized in explosive shock experiments [58]. The simulated XRD of $I\bar{4}3d$ is also presented in Fig. S3 [39].

In Fig. 2, we present a scatter plot of the PBE-based relative total energies (eV/atom) against equilibrium volume ($Å^3$) of the carbon *Pbam*-32, *P*6/*mmm*, and $I\bar{4}3d$ and the previously proposed sp^3 carbons in the past decades, including those deposited in SACADA [4] and those uncovered in our recent stochastic search [5]. *Pbam*-32, *P*6/*mmm*, and $I\bar{4}3d$ show relatively low energies for the carbon family. As summarized in Table I and Table S2, we can see that the total energies of the carbon version *Pbam*-32, *P*6/*mmm*, and $I\bar{4}3d$ relative to cd are 96, 131,

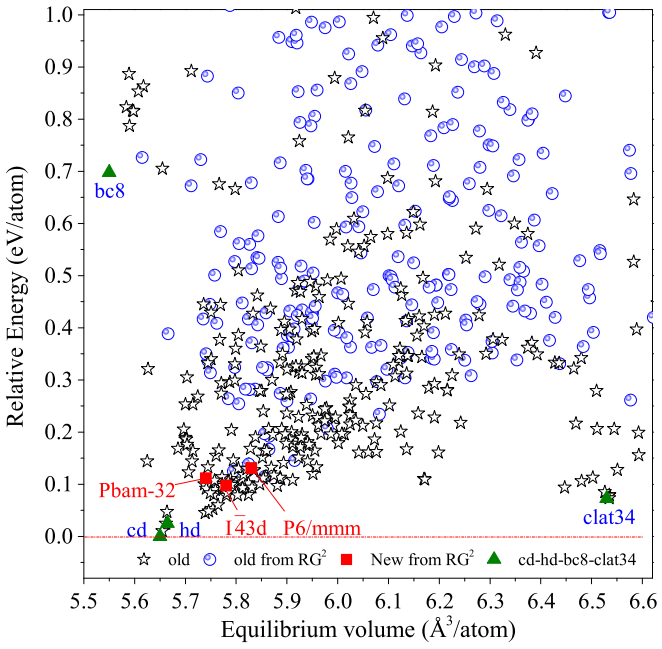

FIG. 2. Scatterplot of the PBE-based relative average energy (eV/atom) against equilibrium volume (Å^3) of the carbon version *Pbam*-32, *P*6/*mmm*, and $I\bar{4}3d$ predicted in this work (red squares), the sp^3 carbons previously predicted in the past decades [4] (black five-point stars), as well as those sp^3 carbons discovered in our recent stochastic search [5] (blue circles). Some well-known carbon phases (green triangles) are also plotted in for comparison.

and 124 meV/atom, respectively, which indicate that they possess good stabilities comparable to the previously proposed *Pbam*-24 (69 meV/atom) [16], *P*41212 (135 meV/atom) [16], *P*42/*ncm* (108 meV/atom) [15], *P*6522 (109 meV/atom) [14], clat46 (106 meV/atom) [17], and Clat34 (73 meV/atom) [17]. In particular, $I\bar{4}3d$ is noted as the third most stable cubic phase among those previously proposed, following clat34 (73 meV/atom) and clat46 (106 meV/atom). It is more stable than the experimentally synthesized *T* carbon (1173 meV/atom) [19,20] and C22 (323 meV/atom) [10,58]. As show in Fig. S4(a), the PBE-based enthalpy-pressure relations for *Pbam*-32, *P*6/*mmm*, and $I\bar{4}3d$ as carbon show that they keep good stability at high pressure in comparison with some well-known carbon phases [39].

The energetic stabilities of *Pbam*-32, *P*6/*mmm*, and $I\bar{4}3d$ as carbon indicate that they possess relatively higher probabilities to be synthesized. However, their dynamical stabilities and elastic stabilities should be determined. The phonon dispersions of *Pbam*-32, *P*6/*mmm*, and $I\bar{4}3d$ as carbon are computed (see methods in the Supplemental Material [39]) and plotted in Fig. S5(a). There are no imaginary frequencies in the phonon band structures, which indicate that *Pbam*-32, *P*6/*mmm*, and $I\bar{4}3d$ are dynamically stable for carbon. The elastic constants for carbon *Pbam*-32, *P*6/*mmm*, and $I\bar{4}3d$ are calculated and summarized in the Supplemental Material [39] in Table S3 together with the corresponding bulk modulus, shear modulus, Young's modulus, and Vicker's hardness [39]. The elastic constants satisfy the mechanical stability criteria for corresponding crystal systems, which indicate that *Pbam*-32, *P*6/*mmm*, and $I\bar{4}3d$ are mechanically stable as carbon. The calculated Vicker' s hardness or bulk modulus of the carbon cd, *Pbam*-32, *P*6/*mmm*, and $I\bar{4}3d$ are 91.32/476.69, 83.58/456.95, 78.45/445.42, and 85.33/443.77 GPa, respectively. These hardness calculations assessed using the empirical Chen's model [59] suggest that the three new carbons are superhard materials [39].

The electronic properties of these three new structures of carbon are investigated by both the PBE and HSE06 methods. The calculated band gaps are summarized in Table I and Table S2 of the Supplemental Material [39] together with those of some selected tetrahedral structures. We can see that the PBE-based band gaps of the carbon *Pbam*-32, *P*6/*mmm*, and $I\bar{4}3d$ are 4.76, 3.55, and 5.91 eV. The band gap of 5.91 eV for $I\bar{4}3d$ is about 0.7 eV larger than that of the previously proposed I-4 (5.25 eV) [60]. It is about 0.93 eV larger than that of *tP*12 (4.98 eV) [61];

TABLE I. The PBE-based total energies ($E_{\rm tot}$: meV/atom) relative to the corresponding cd form, equilibrium volume per atom (V_0: Å^3), and the energy band gaps (indirect and direct) calculated based on PBE ($E_g^{\rm PBE}$: eV) and HSE06 ($E_g^{\rm HSE}$: eV) for various typical phases of carbon, silicon, germanium, and tin.

	C				Si				Ge				Sn			
System	$E_{\rm tot}$	V_0	$E_g^{\rm PBE}$	$E_g^{\rm HSE}$	$E_{\rm tot}$	V_0	$E_g^{\rm PBE}$	$E_g^{\rm HSE}$	$E_{\rm tot}$	V_0	$E_g^{\rm PBE}$	$E_g^{\rm HSE}$	$E_{\rm tot}$	V_0	$E_g^{\rm PBE}$	$E_g^{\rm HSE}$
Pbam-32	98	5.78	4.76/4.89	5.97/6.22	33	20.71	0.81	1.39	31	24.52	0.08	0.66	26	37.33	Metal	0.07
*P*6/*mmm*	131	5.83	3.55/4.75	4.76/5.93	46	20.96	0.56	1.13	46	24.76	0.27	0.77/0.88	39	37.68	Metal	0.40/0.46
$I\bar{4}3d$	112	5.74	5.91	7.24	39	20.44	1.54/1.61	2.19/2.26	35	24.18	0.85/1.06	1.41/1.58	31	36.74	0.47/0.64	0.86/1.03
cd	0	5.65	4.15/5.59	5.32/6.99	0	20.44	0.62/2.56	1.19/3.33	0	24.13	Metal	0.14	0	36.83	Metal	Metal
Pbam-24	68	5.81	4.56/4.79	···	29	20.97	0.85/0.87	···	27	24.83	Metal	···	24	37.81	Metal	···
clat34	73	6.53	3.74/3.77	···	51	23.54	1.38	···	21	27.49	0.59/0.59	···	19	41.76	0.33	···
V carbon	105	5.79	4.44/4.76	···	48	20.65	0.85/1.03	···	45	24.52	Metal	···	35	37.01	Metal	···
clat46	106	6.48	3.85	···	62	23.25	1.31/1.32	···	27	27.21	1.03/1.06	···	23	41.29	0.66/0.67	···
I-4(I1373)	161	6.06	5.25/5.26	6.55/6.56	62	21.72	1.29/1.66	1.91/2.30	52	25.59	1.15/1.21	1.55/1.78	46	38.90	0.73/0.78	1.07/1.19
Si24	235	6.18	2.92/3.60	4.06/4.75	92	21.99	0.51/0.58	1.07/1.13	85	26.05	0.09/0.22	0.59/0.71	74	32.04	0.12/0.25	0.51/0.64
*tp*12(st12)	886	5.59	4.98/5.49	6.27/6.89	166	18.33	1.11/1.39	1.71/1.96	136	21.72	0.25	0.69	60	31.36	Metal	Metal
T carbon	1173	13.18	2.287	···	1024	52.16	Metal	···	943	68.41	Metal	···	792	109.75	Metal	···

therefore $I\bar{4}3d$ is the widest-gap carbon allotrope known. To obtain more reliable band gaps, we then calculate the band structures of cd, I-4, $tP12$, Si24, $Pbam$-32, $P6/mmm$, and $I\bar{4}3d$ using HSE06. The HSE06-based band structures and density of state (DOS) of the carbon $Pbam$-32, $P6/mmm$, and $I\bar{4}3d$ are selected shown in Fig. 3(a). As listed in Table I and Table S2 of the Supplemental Material [39], the HSE06-based band gaps of cd, I-4 [28,60], $tP12$ [61], Si24 [32], $Pbam$-32, $P6/mmm$, and $I\bar{4}3d$ are 5.32, 6.55, 6.27, 4.06, 5.97, 4.76, and 7.24 eV, respectively, which further confirms that $I\bar{4}3d$ is the widest-gap carbon allotrope.

In view of their tetrahedral topological atomic configurations, the crystalline $Pbam$-32, $P6/mmm$, and $I\bar{4}3d$ structures are likely in silicon, germanium, and tin. After optimizing as silicon, germanium, and tin, the topological characteristics of $Pbam$-32, $P6/mmm$, and $I\bar{4}3d$ are maintained. The lattice constants and bond lengths are correspondingly enlarged in comparison with those in carbon and the bond angles are well conserved. We have summarized all the structural information, including space groups, lattice constants, inequivalent atomic positions of $Pbam$-32, $P6/mmm$, and $I\bar{4}3d$, as carbon, silicon, germanium, and tin structures, in the tables in the Supplemental Material [39].

The total energies, equilibrium volumes, PBE-based, and HSE06-based band gaps of the $Pbam$-32, $P6/mmm$, and $I\bar{4}3d$ as silicon, germanium, and tin are summarized in Table I and Table S2 of the Supplemental Material [39]. The total energies of the silicon-version $Pbam$-32, $P6/mmm$, and $I\bar{4}3d$ relative to cd silicon are 33, 46, and 39 meV/atom, respectively. These energies are comparable to those of the previously proposed $Pbam$-24 (29 meV/atom) [16], $P41212$ (39 meV/atom) [16], $P42/ncm$ (44 meV/atom) [15], and $P6522$ (53 meV/atom) [14]. Especially, the silicon version $Pbam$-32, $P6/mmm$, and $I\bar{4}3d$ are more stable than the experimentally viable cage structures Si24 (91 meV/atom) [32], clat34 (51 meV/atom), and clat46 (62 meV/atom), which are highly expected to be synthesized in the future. Both germanium and tin $Pbam$-32, $P6/mmm$, and $I\bar{4}3d$ possess good energetic stabilities. For germanium, the total energies relative to cd germanium are 31, 46, and 35 meV/atom, respectively. For tin, the relative total energies are 26, 39, and 31 meV/atom, respectively. The plotted PBE-based enthalpy-pressure relations for these three new structures and some selected old structures as silicon [Fig. S4(b)], germanium [Fig. S4(c)], and tin [Fig. S4(d)] show that $Pbam$-32, $P6/mmm$, and $I\bar{4}3d$ possess good stability at high pressure.

As shown in Fig. S5 [39], the calculated phonon spectra indicate that $Pbam$-32, $P6/mmm$, and $I\bar{4}3d$ are also dynamically stable for silicon, germanium, and tin. The elastic constants summarized in the Supplemental Material [39] for $Pbam$-32, $P6/mmm$, and $I\bar{4}3d$ as silicon (Table S4), germanium (Table S5), and tin (Table S6) also satisfy the corresponding mechanical stability criteria, indicating that they are also mechanically stable phases for silicon, germanium, and tin. The Vicker's hardness assessed using Chen's empirical model [59] summarized in Tables S4–S6 suggest that silicon, germanium, and tin with structures of $Pbam$-32, $P6/mmm$, and $I\bar{4}3d$ possess similar Vicker's hardness to those in the cd structure.

The electronic properties of these three new structures as silicon, germanium, and tin are also investigated by both

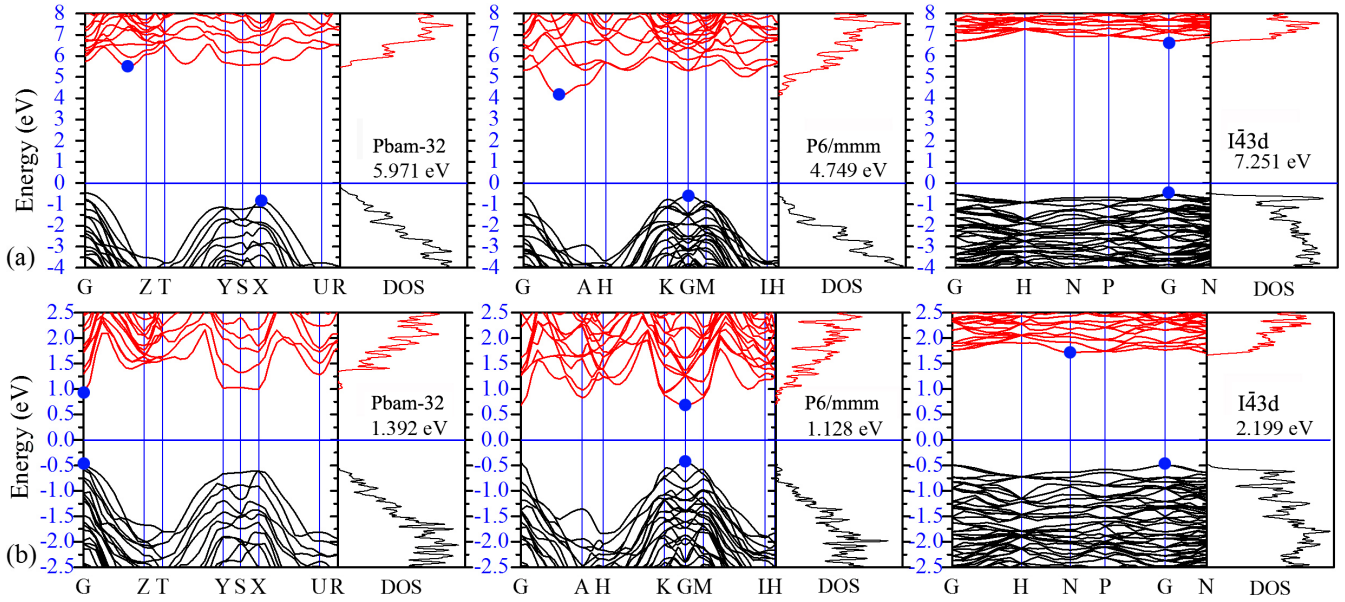

FIG. 3. The HSE06-based electronic band structures and density of states (DOS) of the newly discovered $Pbam$-32, $P6/mmm$, and $I\bar{4}3d$ structures as carbon (a) and silicon (b) at zero pressure.

the PBE and HSE06 methods. Their corresponding band gaps are summarized in Table I and Table S2 of the Supplemental Material [39]. The HSE06-based band structures and density of states of these three structures (*Pbam*-32, *P*6/*mmm*, and $I\bar{4}3d$) for silicon are shown in Fig. 3(b). As silicon, *Pbam*-32 possesses a PBE-based direct band gap of 0.81 eV and a HSE06-based direct band gap of 1.39 eV. The PBE-based gap of *P*6/*mmm* is 0.56 eV and its corresponding HSE06 gap is 1.13 eV. The HSE06-based band gaps of *Pbam*-32 and *P*6/*mmm* are considerably closer to the optimal value of 1.5 eV for photovoltaic applications, similar to that of the recently synthesized Si24 [32]. The silicon $I\bar{4}3d$ structure, has PBE and HSE06 indirect band gaps of 1.54 and 2.19 eV, respectively. The silicon $I\bar{4}3d$ possesses the largest band gap among these selected structures.

The germanium *Pbam*-32 structure possesses a direct PBE band gap of 0.08 eV. This band gap is 0.66 eV in HSE06 as shown in Fig. S6(c) [39]. *P*6/*mmm* germanium is a direct band gap semiconductor (0.27 eV) with the PBE method. However, it becomes a quasidirect band gap semiconductor (0.77/0.88 eV) under HSE06. The $I\bar{4}3d$ germanium is a quasidirect band gap semiconductor with PBE-based and HSE06-based indirect band gaps of 0.85 and 1.41 eV, respectively. These indirect band gaps are slightly smaller than the corresponding direct band gaps of 1.06 and 1.58 eV. The HSE06 band structures and density of states of the tin *Pbam*-32, *P*6/*mmm*, and $I\bar{4}3d$ structures are provided in Fig. S6(d) [39]. The tin-version *Pbam*-32 and *P*6/*mmm* structures are metals within PBE, similar to the cd structure. However, they are narrow band gap semiconductors within HSE06, with gaps of 0.07 and 0.4 eV, respectively. The $I\bar{4}3d$ tin structure is an indirect band gap semiconductor, its PBE-based band gap is 0.47 eV, which will increases to be 0.86 eV in HSE06. These gaps indicate that the tin version $I\bar{4}3d$ is a medium band gap semiconductor, similar to the previously proposed Si24 [32] and *I*-4 [28,60] structures.

In summary, three tetrahedral networks (*Pbam*-32, *P*6/*mmm*, and $I\bar{4}3d$) uncovered by a stochastic search strategy using the AIRSS and RG^2 codes, are investigated as carbon, silicon, germanium, and tin structures through first-principles computations. The newly identified *Pbam*-32, *P*6/*mmm*, and $I\bar{4}3d$ structures contain 32, 36, and 94 atoms in their primitive cells, respectively. For carbon, their energies relative to cd are 96, 131, and 112 meV/atom, respectively, showing good energetic stability. They are further confirmed to be dynamically and elastically stable superhard insulators, which are expected to be synthesized experimentally. $I\bar{4}3d$ is a wide-gap semiconductor with a 7.25 eV gap, which is the widest know band gap of any carbon solid. These three new structures are also confirmed to be viable phases for silicon, germanium, and tin, also showing remarkable energetic stability and positive dynamical and elastic stabilities. Their calculated electronic properties are suitable for semiconductor and photovoltaic applications.

This work is supported by the National Natural Science Foundation of China (Grant No. 11704319), the National Basic Research Program of China (2015CB921103), the Natural Science Foundation of Hunan Province, China (Grant No. 2016JJ3118) and the Program for Changjiang Scholars and Innovative Research Team in University (IRT13093). C. J. P. is supported by the Royal Society through a Royal Society Wolfson Research Merit award and the EPSRC through Grants No. EP/P022596/1 and No. EP/J010863/2.

*hechaoyu@xtu.edu.cn
†cjp20@cam.ac.uk

[1] A. El Goresy and G. Donnay, Science **161**, 363 (1968).
[2] A. G. Whittaker and P. Kintner, Science **165**, 589 (1969).
[3] A. G. Whittaker and G. M. Wolten, Science **178**, 54 (1972).
[4] Sacada, http://sacada.sctms.ru/.
[5] X. Shi, C. He, C. J. Pickard, C. Tang, and J. Zhong, Phys. Rev. B **97**, 014104 (2018).
[6] Q. Li, Y. Ma, A. R. Oganov, H. Wang, H. Wang, Y. Xu, T. Cui, H.-K. Mao, and G. Zou, Phys. Rev. Lett. **102**, 175506 (2009).
[7] A. R. Oganov and C. W. Glass, J. Chem. Phys. **124**, 244704 (2006).
[8] C. He, L. Sun, C. Zhang, X. Peng, K. Zhang, and J. Zhong, Solid State Commun. **152**, 1560 (2012).
[9] D. Li, K. Bao, F. Tian, Z. Zeng, Z. He, B. Liu, and T. Cui, Phys. Chem. Chem. Phys. **14**, 4347 (2012).
[10] C. He, C. Zhang, H. Xiao, L. Meng, and J. Zhong, Carbon **112**, 91 (2017).
[11] F. J. Ribeiro, P. Tangney, S. G. Louie, and M. L. Cohen, Phys. Rev. B **74**, 172101 (2006).
[12] W. L. Mao, H.-k. Mao, P. J. Eng, T. P. Trainor, M. Newville, C.-c. Kao, D. L. Heinz, J. Shu, Y. Meng, and R. J. Hemley, Science **302**, 425 (2003).
[13] K. Yamada, Carbon **41**, 1309 (2003).
[14] C. J. Pickard and R. J. Needs, Phys. Rev. B **81**, 014106 (2010).
[15] Z. Zhao, F. Tian, X. Dong, Q. Li, Q. Wang, H. Wang, X. Zhong, B. Xu, D. Yu, J. He *et al.*, J. Am. Chem. Soc. **134**, 12362 (2012).
[16] A. Mujica, C. J. Pickard, and R. J. Needs, Phys. Rev. B **91**, 214104 (2015).
[17] G. Benedek, E. Galvani, S. Sanguinetti, and S. Serra, Chem. Phys. Lett. **244**, 339 (1995).
[18] X. Yang, M. Yao, X. Wu, S. Liu, S. Chen, K. Yang, R. Liu, T. Cui, B. Sundqvist, and B. Liu, Phys. Rev. Lett. **118**, 245701 (2017).
[19] X.-L. Sheng, Q.-B. Yan, F. Ye, Q.-R. Zheng, and G. Su, Phys. Rev. Lett. **106**, 155703 (2011).
[20] J. Zhang, R. Wang, X. Zhu, A. Pan, C. Han, X. Li, D. Zhao, C. Ma, W. Wang, H. Su *et al.*, Nat. Commun. **8**, 683 (2017).
[21] B. Haber, T. A. Strobel, and J. E. Bradby, Appl. Phys. Rev. **3**, 040808 (2016).

[22] W. Stefan, H. Yuping, M. Vörös, and G. Galli, Appl. Phys. Rev. **3**, 040807 (2016).
[23] Y. Liu, X. Jiang, Y. Huang, S. Zhou, and J. Zhao, J. Appl. Phys. **121**, 085107 (2017).
[24] B. D. Malone and M. L. Cohen, Phys. Rev. B **85**, 024116 (2012).
[25] M. Amsler, S. Botti, M. A. L. Marques, T. J. Lenosky, and S. Goedecker, Phys. Rev. B **92**, 014101 (2015).
[26] S. Botti, J. A. Flores-Livas, M. Amsler, S. Goedecker, and M. A. L. Marques, Phys. Rev. B **86**, 121204 (2012).
[27] M. C. Nguyen, X. Zhao, C.-Z. Wang, and K.-M. Ho, Phys. Rev. B **89**, 184112 (2014).
[28] I.-H. Lee, J. Lee, Y. J. Oh, S. Kim, and K. J. Chang, Phys. Rev. B **90**, 115209 (2014).
[29] H. J. Xiang, B. Huang, E. Kan, S.-H. Wei, and X. G. Gong, Phys. Rev. Lett. **110**, 118702 (2013).
[30] Q. Wang, B. Xu, J. Sun, H. Liu, Z. Zhao, D. Yu, C. Fan, and J. He, J. Am. Chem. Soc. **136**, 9826 (2014).
[31] L. Rapp, B. Haberl, C. J. Pickard, J. E. Bradby, E. G. Gamaly, J. S. Williams, and A. V. Rode, Nat. Commun. **6**, 7555 (2015).
[32] D. Y. Kim, S. Stefanoski, O. O. Kurakevych, and T. A. Strobel, Nat. Mater. **14**, 169 (2015).
[33] Z. Zhao, H. Zhang, D. Y. Kim, W. Hu, E. S. Bullock, and T. A. Strobel, Nat. Commun. **8**, 13909 (2017).
[34] C. He, C. Zhang, J. Li, X. Peng, L. Meng, C. Tang, and J. Zhong, Phys. Chem. Chem. Phys. **18**, 9682 (2016).
[35] C. J. Pickard and R. J. Needs, Phys. Rev. Lett. **97**, 045504 (2006).
[36] C. J. Pickard and R. J. Needs, J. Phys. Condens. Matter **23**, 053201 (2011).
[37] Y. Wang, J. Lv, L. Zhu, and Y. Ma, Phys. Rev. B **82**, 094116 (2010).
[38] C. W. Glass, A. R. Oganov, and N. Hansen, Comput. Phys. Commun. **175**, 713 (2006).
[39] See Supplemental Material at http://link.aps.org/supplemental/10.1103/PhysRevLett.121.175701 for the methodology details [40–51] (s1), supplementary figures (s2), and supplementary tables (s3) for some important results of *Pbam*-32, $P6/mmm$, and $I\bar{4}3d$ as carbon, silicon, germanium, and tin.
[40] G. Kresse and J. Furthmüller, Phys. Rev. B **54**, 11169 (1996).
[41] G. Kresse and J. Furthmller, Comput. Mater. Sci. **6**, 15 (1996).
[42] G. Kresse and D. Joubert, Phys. Rev. B **59**, 1758 (1999).
[43] J. P. Perdew, K. Burke, and M. Ernzerhof, Phys. Rev. Lett. **77**, 3865 (1996).
[44] A. Togo, F. Oba, and I. Tanaka, Phys. Rev. B **78**, 134106 (2008).
[45] J. Heyd, G. E. Scuseria, and M. Ernzerhof, J. Chem. Phys. **118**, 8207 (2003).
[46] Y. Le Page and P. Saxe, Phys. Rev. B **65**, 104104 (2002).
[47] R. Hill, Proc. Phys. Soc. London Sect. A **65**, 349 (1952).
[48] F. Gao, J. He, E. Wu, S. Liu, D. Yu, D. Li, S. Zhang, and Y. Tian, Phys. Rev. Lett. **91**, 015502 (2003).
[49] P. E. Blöchl, Phys. Rev. B **50**, 17953 (1994).
[50] A. Togo, computer code phonopy, https://atztogo.github.io/phonopy/, 2016.
[51] J. F. Nye, *Physical Properties of Crystals* (Clarendon Press, Oxford, 1964).
[52] M. D. Segall, P. J. D. Lindan, M. J. Probert, C. J. Pickard, P. J. Hasnip, S. J. Clark, and M. C. Payne, J. Phys. Condens. Matter **14**, 2717 (2002).
[53] Z. Whang, Y. Zhao, K. Tait, X. Liao, D. Schiferl, C. Zha, R. T. Downs, J. Qian, Z. Yuntian, and T. Shen, Proc. Natl. Acad. Sci. U.S.A. **101**, 13699 (2004).
[54] M. Hu, Z. Zhao, F. Tian, A. R. Oganov, Q. Wang, M. Xiong, C. Fan, B. Wen, J. He, D. Y. Yu *et al.*, Sci. Rep. **3**, 1331 (2013).
[55] X. Dong, M. Hu, J. He, Y. Tian, and H.-T. Wang, Sci. Rep. **5**, 10713 (2015).
[56] C. He and J. Zhong, Solid State Commun. **181**, 24 (2014).
[57] A. El Goresy, L. S. Dubrovinsky, P. Gillet, S. Mostefaoui, G. Graup, M. Drakopoulos, A. S. Simionovici, V. Swamy, and V. L. Masaitis, C. R. Geoscience **335**, 889 (2003).
[58] K. Yamada, Carbon **41**, 1309 (2003).
[59] X. Chen, H. Niu, D. Li, and Y. Li, Intermetallics **19**, 1275 (2011).
[60] X. Zhang, Y. Wang, J. Lv, C. Zhu, Q. Li, M. Zhang, Q. Li, and Y. Ma, J. Chem. Phys. **138**, 114101 (2013).
[61] Q. Zhu, A. R. Oganov, M. A. Salvadó, P. Pertierra, and A. O. Lyakhov, Phys. Rev. B **83**, 193410 (2011).